Physiologically Based Pharmacokinetic Models for Trichloroethylene and Its Oxidative Metabolites

Jeffrey W. Fisher

Air Force Research Laboratory, Operational Toxicology Branch, Human Effectiveness Directorate, Wright-Patterson AFB, Ohio USA

Trichloroethylene (TCE) pharmacokinetics have been studied in experimental animals and humans for over 30 years. Compartmental and physiologically based pharmacokinetic (PBPK) models have been developed for the uptake, distribution, and metabolism of TCE and the production, distribution, metabolism, and elimination of P450-mediated metabolites of TCE. TCE is readily taken up into systemic circulation by oral and inhalation routes of exposure and is rapidly metabolized by the hepatic P450 system and to a much lesser degree, by direct conjugation with glutathione. Recent PBPK models for TCE and its metabolites have focused on the major metabolic pathway for metabolism of TCE (P450-mediated metabolic pathway). This article briefly reviews selected published compartmental and PBPK models for TCE. Trichloroacetic acid (TCA) is considered a principle metabolite responsible for TCE-induced liver cancer in mice. Liver cancer in mice was considered a critical effect by the U.S. Environmental Protection Agency for deriving the current maximum contaminant level for TCE in water. In the literature both whole blood and plasma measurements of TCA are reported in mice and humans. To reduce confusion about disparately measured and model-predicted levels of TCA in plasma and whole blood, model-predicted outcomes are compared for first-generation (plasma) and second-generation (whole blood) PBPK models published by Fisher and colleagues. Qualitatively, animals and humans metabolize TCE in a similar fashion, producing the same metabolites. Quantitatively, PBPK models for TCE and its metabolites are important tools for providing dosimetry comparisons between experimental animals and humans. TCE PBPK models can be used today to aid in crafting scientifically sound public health decisions for TCE. *Key words*: chloral hydrate, dichloroacetic acid, human, metabolism, PBPK models, pharmacokinetics, rodents, trichloroacetic acid, trichloroethanol, trichloroethylene. — *Environ Health Perspect* 108(suppl 2):265–273 (2000).
http://ehpnet1.niehs.nih.gov/docs/2000/suppl-2/265-273fisher/abstract.html

Pharmacokinetic Modeling and Trichloroethylene

Trichloroethylene (TCE) is now a widespread environmental contaminant in the United States because of its historical use as a degreaser in the 1960s and 1970s. Occupational health concerns for TCE vapors began in the 1970s in Europe and the United States, which prompted the publication of two human pharmacokinetic models for TCE. The utility of human pharmacokinetic models was recognized at this time as a tool to quantify individual exposure to TCE vapor. Sato et al. (*1*) published a 3-compartment human model to describe the systemic clearance of TCE from blood and the urinary excretion of metabolites (trichloroacetic acid [TCA] and trichloroethanol [TCOH]). Pharmacokinetic data were collected from four male Japanese students who were exposed to 100 ppm of TCE for 4 hr. Fernandez et al. (*2*) published a 5-compartment human model based on controlled human exposures to TCE vapors for 8 hr ranging from 54 to 160 ppm. TCE in exhaled breath and the cumulative amount of TCA and TCOH excreted in urine were simulated with this 5-compartment model. Since the publication of these two human pharmacokinetic models for TCE, several animal and human pharmacokinetic models for TCE and its metabolites have been published.

Qualitatively, animals and humans handle the uptake, distribution, metabolism, and elimination of TCE in a similar fashion. This is a very appealing situation for animal-to-human extrapolation of TCE dosimetry based on validated animal physiologically based pharmacokinetic (PBPK) models for TCE. Usually cost and ethical concerns limit the amount of pharmacokinetic data that may be obtained in human volunteers, placing the burden of PBPK model development on animal studies. In addition, animal toxicity studies are usually employed to assess the human health hazard potential of chemicals such as TCE. Several rodent and human PBPK models were published for TCE and in some cases these models were used in cancer and non-cancer risk predictions. Andersen et al. (*3*) collected pharmacokinetic data in rats and developed a 4-compartment PBPK model for TCE in rats. Metabolic capacity was estimated in the rats by predicting atmospheric loss of TCE in a gas uptake chamber. This was a landmark physiological model for TCE because the nonlinear kinetic behavior of TCE was quantitatively described with Michaelis-Menten metabolic parameters. This provided the ability for a PBPK model to predict TCE blood and tissue time courses over a wide range of exposure concentrations or doses, corresponding to flow- and capacity-limited metabolism of TCE. Dallas et al. (*4*) incorporated the metabolic parameter estimates published by Andersen et al. (*3*) in a 4-compartment PBPK rat model. Detailed kinetic time-course studies of exhaled breath and blood were conducted with rats. Bogen (*5*) was interested in using a PBPK model for TCE to predict human health risks associated with environmental exposure to TCE. He performed a kinetic analysis with TCE using simplified steady-state equations to predict human health risks for cancer based on the amount of TCE metabolized. At this time, the U.S. Environmental Protection Agency (U.S. EPA) released a risk assessment for TCE that relied on the estimated amounts of TCE metabolized in animal and human studies (*6*). Koizumi (*7*) also predicted human health risks at steady state using a 4-compartment PBPK model and simulated the amount of TCE metabolized in rats and humans. Koizumi collected a limited amount of kinetic data for consumption of TCE dissolved in water.

More elaborate rodent PBPK models for TCE were developed to include TCA, a major metabolite of TCE. Understanding the dosimetry of TCA was thought important because of emerging animal toxicity findings with TCA stemming from identification of TCA as a byproduct of water chlorination. Fisher et al. (*8,9*) collected pharmacokinetic data and developed PBPK pregnancy and lactation models to assess placental and lactational transfer of TCE and TCA in rats administered TCE in drinking water, by gavage, and as vapors (inhalation). A 7-compartment pregnancy PBPK model was developed to describe TCE in maternal blood and near-term fetal blood (*8*). A linked 3-compartment submodel was used to describe TCA in maternal and near-term fetal plasma. Transfer of TCE from the maternal side of the placenta to the fetus was described with fetal

This article is part of the monograph on Trichloroethylene Toxicity.

Address correspondence to J.W. Fisher, Air Force Research Laboratory, Operational Toxicology Branch, Human Effectiveness Directorate, 2856 G St., Bldg. 79, Wright-Patterson AFB, OH 45433. Telephone: (937) 255-5150, ext. 3108. Fax: (937) 255-1474. E-mail: jeffrey.fisher@wpafb.af.mil

This review was funded by the Strategic Environmental Research and Development Program (SERDP) and supported by the U.S. Air Force under contract F41624-96-C-9010.

Received 20 October 1999; accepted 25 February 2000.

blood flow to the placenta. TCA transfer from the placenta to the fetus was described as a diffusion-limited process. Both TCE and TCA concentrations in near-term fetal blood and plasma, respectively, were somewhat lower than circulating maternal blood and plasma concentrations of TCE and TCA for oral gavage, inhalation, and drinking water routes of exposure to TCE. Fisher et al. (*9*) then developed a 5-compartment PBPK model to describe TCE in maternal blood and milk, which was linked with a 4-compartment model to describe deposition of TCE in a nursing pup. TCA in maternal plasma and milk was described with a 3-compartment submodel and TCA in pup plasma was described with a linked 1-compartment submodel. Transfer of TCE into the milk compartment was described with a venous equilibration equation and transfer of TCA from the mammary tissue into milk was described as a diffusion-limited process. TCE concentrations in milk were higher than corresponding maternal blood concentrations and TCA concentrations in milk were lower than corresponding maternal plasma TCA concentrations. These PBPK models demonstrated the ability of experimentally validated PBPK models to simulate maternally mediated fetal (placental transfer) and neonatal (lactational transfer) dosimetry of TCE and TCA for different routes of maternal exposure to TCE.

In subsequent PBPK modeling efforts, referred to as first-generation models, with mice, rats, and humans, Fisher and colleagues focused on the development and validation of PBPK models for TCE and TCA, with the majority of the research effort focused on $B6C3F_1$ mice. TCE-induced liver cancer in the $B6C3F_1$ mouse was a critical end point for the existing 1985 U.S. EPA risk assessment for TCE (*6*) and was thought to be important in future risk assessment activities by the U.S. EPA. Researchers in the late 1980s demonstrated that TCA and dichloroacetic acid (DCA) administered in drinking water caused liver tumors in $B6C3F_1$ mice (*10*). TCA is a major metabolite of TCE and was thought by Fisher and colleagues to be the primary carcinogen responsible for TCE-induced liver tumors in mice, while DCA was a thought to be a very minor metabolite. First-generation PBPK models were developed for TCE and TCA in male and female mice (*11,12*) and male and female rats (*11*) exposed to TCE vapors or dosed by gavage with TCE. Allen and Fisher (*13*) published a human PBPK model for TCE and TCA using previously published pharmacokinetic studies in humans with TCE and its metabolites. These models described TCE in blood of mice, rats, and humans; TCE in exhaled breath of humans; and TCA in plasma of mice, rats, and humans. These first-generation mice and human PBPK models for TCE and TCA will be discussed in detail.

The most recent advancements in PBPK modeling of TCE and its metabolites occurred in mice and humans (*14–16*). In the mouse, pharmacokinetic studies were undertaken in the laboratory to support development and validation of second-generation PBPK models for P450-mediated metabolism of TCE to chloral hydrate (CH), DCA, TCA, TCOH, and trichloroethanol glucuronide (TCOH-b) (*14,15*). A human PBPK model was developed using new pharmacokinetic data collected from eight females and nine males that were exposed to TCE vapors (50 or 100 ppm) for 4 hr in a chamber (*16*). Blood, urine, and limited exhaled breath samples were collected to support construction of this PBPK model for TCE, TCA, and TCOH (*16*). These second-generation PBPK models will be discussed in detail.

Many of the toxic and carcinogenic properties of TCE result from metabolism of TCE (*6*). A key determinant in elucidating dose–response relationships for TCE is quantifying the pharmacokinetics of the major metabolites of TCE. The use of PBPK models in risk assessment is appealing because these models can be used to estimate target-organ dose of metabolites in experimental animals and humans. Five risk assessments have been recently published for TCE using PBPK models for TCE and its P450-mediated metabolites and glutathione conjugate. Fisher and Allen (*12*) calculated human health risks for liver cancer using previously published mice and human PBPK models. Cronin et al. (*17*) conducted a Monte Carlo simulation of the PBPK risk assessment models reported by Fisher and Allen (*12*). Clewell et al. (*18*) published the results of a PBPK risk analysis for lung and liver cancers based on P450-mediated metabolites and kidney cancer based on conjugation of TCE with glutathione. No details of their PBPK model structure were provided for the glutathione metabolic pathway. Bogen and Gold (*19*) calculated cancer risks for TCE using PBPK models of Fisher and Allen (*12*) and Allen and Fisher (*13*). Simon (*20*) constructed a 4-compartment stochastic PBPK model for TCE with 1-compartment submodels for TCOH and TCA to predicted blood concentrations of TCOH and TCE that would cause drowsiness in humans.

The objective of this paper is to review and compare recent mice and human PBPK models for TCE and its major P450-mediated metabolites. Two human PBPK models for TCE and its metabolites, Allen and Fisher (*13*) and Fisher et al. (*16*), were selected for review. Mouse PBPK models selected for review were those by Fisher et al. (*11*), Fisher and Allen (*12*), Abbas and Fisher (*14*), and Greenberg et al. (*15*).

PBPK Model Structures for TCE and Its P450-Mediated Metabolites in the $B6C3F_1$ Mouse

The first generation PBPK models for TCE in the male and female $B6C3F_1$ mouse (*11,12*) were 4-compartment models, similar to styrene, reported by Ramsey and Andersen (*21*). The four compartments included fat, liver, and slowly perfused (muscle) and richly perfused tissue groups (Figure 1). TCE is extensively metabolized in the liver by P4502E1, yielding two major metabolites, TCA and TCOH. A simple, classical 1-compartment model was used to describe the kinetics of one metabolite, TCA. A proportionality constant (PO) was used to describe the stoichiometric yield of TCA based on the simulated amount of TCE that was metabolized (Figure 1). The differential equations used to describe the compartments are found in Fisher et al. (*11*) and Fisher and Allen (*12*).

The second-generation PBPK models for TCE in male $B6C3F_1$ mice (*14–16*) were 6-compartment models consisting of fat, liver, kidney, lung, and slowly perfused (muscle) and richly perfused tissue groups (Figure 2A). In addition to the metabolite TCA, other P450-mediated metabolites (CH, DCA, TCOH, and TCOH-b) were included

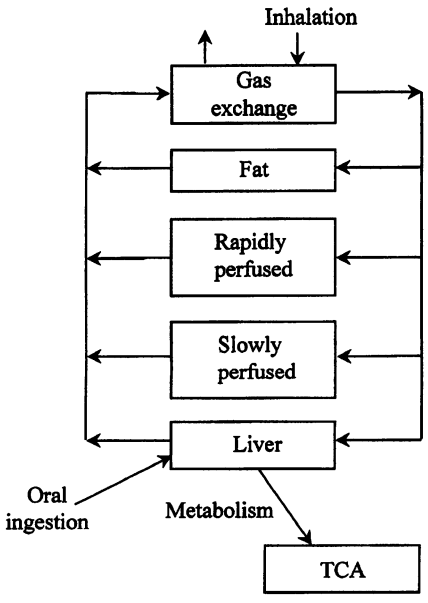

Figure 1. Schematic of first-generation PBPK model for TCE and its oxidative metabolite in mice (*11,12*) and humans (*13*). TCE is inhaled or ingested in drinking water and for mice administered by oral bolus gavage. TCE distributes into the body compartments and is either metabolized in the liver to TCA or exhaled in breath.

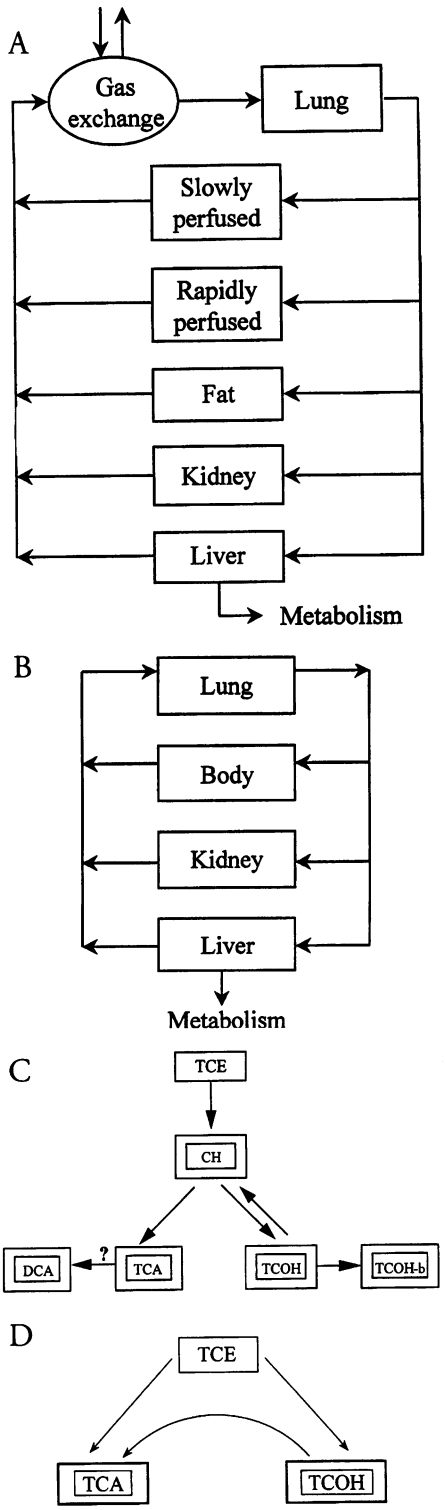

Figure 2. (*A*) Schematic of second-generation PBPK model for TCE in mice (*14,15*) and humans (*16*). TCE is inhaled and for mice it is administered by oral bolus gavage. (*B*) Schematic of second-generation PBPK subcompartment model structure for metabolites of TCE, including CH, TCA, DCA, free TCOH (TCOH), and bound TCOH (TCOH-b) in mice and TCA and TCOH in humans. (*C*) Schematic of second-generation PBPK model subcompartment linkages for metabolic pathway of TCE in mice. (*D*) Schematic of second-generation PBPK model subcompartment linkages for metabolic pathway of TCE in humans.

in the second-generation PBPK models. Each metabolite was described by a 4-compartment PBPK submodel (Figure 2B), which included the lung, liver, kidney, and the body. The liver was included in the submodel structure because of its role in metabolism and as a target organ for tumor formation in $B6C3F_1$ mice after chronic oral administration of TCE (*6*). The lung was included in the submodel structure because the lung is a target organ for tumor formation in $B6C3F_1$ mice after chronic exposure to TCE vapors (*22*). The kidney's role in the submodel structure was urinary excretion of metabolites and assessing metabolite dosimetry. The differential equations used to describe the submodel compartments are found in Abbas and Fisher (*14*) and Greenberg et al. (*15*).

The linkage of the metabolite submodels (Figure 2C) was based on a proposed pathway for metabolism of TCE taken from Davidson and Beliles (*23*). The first metabolic step is oxidation of TCE and is the rate-limiting step in the metabolism of TCE. Subsequent rearrangement of TCE after insertion of the oxygen yields a reactive intermediate, trichloroacetaldehyde, which is then hydrolyzed to form CH. CH is either reduced by alcohol dehydrogenase and aldehyde reductase in the liver to TCOH or oxidized by aldehyde dehydrogenase in the liver to TCA. In the male $B6C3F_1$ mouse, a small fraction of TCOH is converted to CH, presumably by alcohol dehydrogenase, and apparently a small fraction of TCA is dechlorinated in the liver to yield DCA. In male $B6C3F_1$ mice, DCA is rapidly metabolized in the liver to nonchlorinated acids (oxalate, glyoxalate, and glycolate) and monochloroacetic acid (*24*). The majority of free TCOH is conjugated with TCOH-b, which is excreted in urine and feces. The differential equations used to describe the compartments are found in Abbas and Fisher (*14*) and Greenberg et al. (*15*).

A key difference between the first- and second-generation PBPK mice models for TCE and its oxidative metabolites was that PO values were not used to describe the yield of metabolites in the second-generation PBPK models. In the second-generation mouse model, all of the metabolized TCE was converted to CH at a rate equal to the rate of oxidation of TCE. First-order rate constants were then used to describe the metabolic conversion of CH→TCA, TCA→DCA, TCOH→CH, and a saturable nonlinear term was used to describe TCOH→TCOH-b. First-order terms were used to describe urinary excretion of CH, TCA, TCOH, and TCOH-b and fecal elimination of TCOH-b.

Derivation of PBPK Model Parameters for Mice

Physiological values (e.g., blood flows and tissue and organ volumes) for the first- and second-generation PBPK model compartments were taken from the literature or calculated when organs or tissues were grouped as one compartment (Table 1). Chemical-specific model parameters, such as partition coefficients (Table 2), metabolic rate constants, and urinary excretion rate constants (Table 3) were determined experimentally in separate studies or by using pharmacokinetic time-course data from experiments that were used to construct and validate the PBPK models. Fitted rate constant values were determined by

Table 1. Compartment volumes, blood flows, cardiac output, alveolar ventilation, and body weight values used in the first- and second-generation PBPK mice models for TCE.

Physiological parameter	First-generation mouse model		Second-generation mouse model
	Female	Male	Male
Compartment volumes (% bw)			
Liver	4.0	4.0	4.0
Lung	–[a]	–[a]	0.66
Kidney	–[a]	–[a]	1.8
Slowly perfused	72.0	78.0	72.0
Richly perfused	5.0	5.0	3.0
Fat	10	4.0	10.0
Body (for metabolites)	–[a]	–[a]	82.0
Blood flow (% CO)			
Liver	24.0	24.0	24.0
Lung	–[a]	–[a]	100.0
Kidney	–[a]	–[a]	9.0
Slowly perfused	19.0	19.0	19.0
Richly perfused	52.0	52.0	43.0
Fat	5.0	5.0	5.0
Body (for metabolites)	–[a]	–[a]	24.0
Alveolar ventilation (L/hr/kg)	30.0	30.0	28.0
Cardiac output (L/hr/kg)	30.0	30.0	11.6
Body weight (kg)	0.023–0.030	0.029–0.033	0.025–0.031

[a]Compartment was not included in the first-generation PBPK model for mice.

Table 2. Blood/air and tissue/blood partition coefficient values for TCE in first- and second-generation PBPK mice models.

	First-generation mouse model		Second-generation mouse model					
	Female	Male	Male					
Partition coefficient	TCE	TCE	TCE	CH	TCOH	TCOH-b	TCA	DCA
Blood/air	14.3	13.4	15.9	–	–	–	–	–
Liver/blood	1.6	2.0	1.7	1.4	1.3	0.6	1.2	1.1
Fat/blood	31.4	41.3	36.4	–	–	–	–	–
Richly perfused/blood	1.6	2.0	1.7	–	–	–	–	–
Kidney/blood	–[a]	–[a]	2.1	1.0	1.0	1.4	0.7	0.7
Slowly perfused/blood	0.5	1.0	2.4	1.4	1.1	1.1	0.9	0.4
Lung/blood	–[a]	–[a]	2.61	1.7	0.8	1.1	0.5	1.2

[a]Compartment was not included in first-generation mouse model for TCE.

Table 3. Chemical-specific model parameters in mice for first- and second-generation PBPK models.

	First-generation mouse model		Second-generation mouse model (male)	
Model parameters	Female	Male	Oral	Inhalation
Oral uptake rate constant for TCE (/hr)	0.9	1.1	3.9[a]	
			2.18	
			0.44	
TCA (1 compartment)				
Oral				
Volume of distribution for TCA (L/kg)	0.176	0.238		
Plasma elimination rate constant (/hr)	0.062	0.028		
PO (fractional yield of TCA, unitless)	0.09	0.06		
Inhalation				
Volume of distribution (L)	0.176	0.236		
Plasma elimination rate constant (/hr)	0.104	0.043		
PO (fractional yield of TCA, unitless)	0.07–0.18	0.07–0.13		
TCE				
Maximum rate of TCE→CH (mg/hr-kg)	23.2	32.7	32.7	32.7
Michaelis-Menten constant (mg/L)	0.25	0.25	4.61	0.25
Fractional uptake of inhaled TCE vapor	–	–	–	0.53
CH				
First-order rate, CH→TCOH (/hr/kg)			309	412.39
First-order rate, CH→TCA (/hr/kg)			115	187.75
First-order urinary excretion of CH (/hr/kg)			.06	0.06
TCOH				
Maximum rate of TCOH glucuronidation (mg/hr-kg)			16.5	33.16
Michaelis-Menten constant (mg/L)			15.7	9.47
First-order rate, TCOH→CH (/hr/kg)			1.32	1.54
First-order urinary excretion of TCOH (/hr/kg)			1.14	1.14
TCOH-b				
First-order urinary excretion of TCOG (/hr/kg)			32.8	32.8
First-order excretion of TCOG in feces (/hr/kg)			4.61	4.61
TCA				
First-order TCA→DCA (/hr/kg)			0.35	0.0036
First-order urinary excretion of TCA (/hr/kg)			1.55	2.50
DCA				
First-order DCA→other metabolites (/hr/kg)			20.5	1.05

[a]Two first-order rate constants (3.9 and 0.44/hr) described the uptake of TCE into the liver and a first-order rate (2.18/hr) described the transfer of TCE from the first to second compartment.

optimization or manually adjusting model rate constant values until agreement was reached between predicted and observed pharmacokinetic data using Simusolv (Dow Chemical Company, Midland, MI) or ACSL (MGA, Inc., Boston, MA).

The vial-equilibrium method (*25*) was used to determine *in vitro* tissue/air and blood/air partition coefficient (PC) values for TCE (Table 2). For the first-generation PBPK model for male and female B6C3F$_1$ mice, F344 rat tissue/air PC values and male and female mice blood/air PC values were measured and used as estimates of tissue/blood PC values for male and female B6C3F$_1$ mice. Mice tissues and blood were used to determine TCE tissue/air and blood/air PC values for the second-generation PBPK models with the exception of using a rat liver/air PC value.

A nonvolatile method (*26*) was used to determine *in vitro* tissue/blood partition coefficients for TCE metabolites (Table 2) for use in the second-generation PBPK model. Estimates of TCOH-b tissue/blood PC values for liver, kidney, lung, and muscle (Table 2) were determined *in vivo* from terminal blood and tissue concentration time-course data for TCOH-b after oral administration of 1,200 mg/kg of TCE.

Gas-uptake methodology was employed to estimate the *in vivo* metabolic capacity for oxidation of TCE in B6C3F$_1$ mice (Table 3). A series of atmospheric loss curves were generated for male and female B6C3F$_1$ mice, ranging from 300 to 10,000 ppm initial concentrations, and analyzed using the first PBPK model for TCE to estimate the Michaelis-Menten constants, V_{maxc} and K_m. The V_{maxc} values for male and female mice were 32.7 and 23.2 mg/kg/hr, respectively, scaled to bw$^{0.7}$. The K_m value was estimated to be 0.25 mg/L for both male and female mice. The V_{maxc} value obtained in the first-generation model for male mice was used in the second-generation models. However, Abbas and Fisher (*14*) adjusted the value of K_m to a value of 4.6 mg/L to provide an adequate fit of the blood–time-course data for TCE. The adjustment of the K_m value for TCE is disconcerting, since the only other reported value for K_m is 0.25 mg/L (Table 3). This adjustment in K_m value reflects the difficulty in describing TCE blood–time-course data for mice dosed by oral intubation with TCE dissolved in corn oil. There is no reason to suspect that corn oil alters the K_m value for oxidation of TCE; rather this adjustment in K_m reflects an oversimplification of the model structure for describing oral uptake of TCE dissolved in corn oil. In the first-generation PBPK model, TCE blood–time-course data for mice dosed with TCE dissolved in corn oil could not be described with a single oral uptake rate constant. In the second-generation PBPK model, TCE blood–time-course data were adequately described using two oral uptake rate constants representing both rapid and slow oral uptake phases (Table 3) and increasing the K_m value from 0.25 to 4.6 mg/L.

Intravenous (i.v.) dosing studies (100 mg/kg) with CH, TCOH, TCA, or DCA were initially conducted to estimate apparent metabolic rate constant values for each metabolite (*27*). Metabolic rate constant values for each administered metabolite were estimated by visual fitting of blood–time-course data for the administered chemical and its metabolic products using the submodel structure (Figure 2B) and metabolic pathway linkage (Figure 2C). DCA, TCOH, TCOH-b, and TCA were measured in mice dosed with CH (*28*), but in later experiments DCA was not measured as a metabolite of CH, TCA, or TCOH in male B6C3F$_1$ mice (*29*).

A large number of male B6C3F$_1$ mice were given bolus doses of TCE dissolved in corn oil to construct and validate the oral

dosing second-generation PBPK model (*14*). Blood, tissues, and urine were collected for analysis of TCE and metabolites in four dose groups (2,000, 1,200, 600, and 300 mg/kg). The 1,200-mg/kg dose group was used to develop the PBPK model for TCE and its P450-mediated metabolites. The following rate constants were obtained by adjusting rate constant values until an adequate visual fit of the time-course data could be obtained: urinary rate constant values for CH, TCOH, TCOH-b, and TCA, 2-compartment oral uptake rate constant values for TCE, first-order fecal elimination of TCOH-b, and a first-order metabolic rate constant value for metabolism of DCA. Other metabolic rate constant values in the PBPK model were visually fitted rate constant values taken from i.v. dosing studies (*27*). Abbas and Fisher (*14*) showed measured and model-simulated pharmacokinetic profiles for TCE in blood and fat, TCOH and CH in blood and lung, TCA and DCA in blood and liver, and TCA in urine and TCOH-b in blood and urine. Low concentrations of DCA were measured in mice administered TCE by gavage, and its formation was kinetically described as reductive dechlorination of TCA.

Greenberg et al. (*15*) exposed mice for 4 hr to TCE vapor concentrations of 100 and 600 ppm. Measured and model-predicted time-course concentrations are presented for TCE in blood, TCA in liver and blood, TCOH in blood and lung and TCOH-b in blood, and DCA in blood and liver. Model parameter values were taken from Abbas and Fisher (*14*) or in some cases adjusted to obtain better visual agreement between model simulation and observation (Table 3). In this PBPK model, fractional uptake of TCE (53%) was used to describe inhalation of TCE vapors in mice. Exhaled breath studies were conducted after inhalation of TCE vapors to provide supporting evidence for fractional uptake of TCE in the lung. Model simulations suggested that only about 50% of the inhaled TCE vapor was taken into systemic circulation in the lung in the $B6C3F_1$ mouse.

Table 3 provides a comparison of the second-generation PBPK model parameters for inhalation of TCE vapors (*15*) and oral ingestion of TCE dissolved in corn oil (*14*). The rate constant values for several parameters differ between the two routes of administration. In the inhalation model the rate constant values for formation of TCA and TCOH and for glucuronidation of TCOH to TCOH-b are greater than in the oral dosing model. In addition, rate-constant values associated with formation and metabolism of DCA are less in the inhalation model compared to the oral dosing model. Because of the dynamic nature of a bolus gavage dose and the complexity of oral absorption of TCE dissolved in corn oil, the 4-hr inhalation study provides a more suitable data set for estimating the kinetic rate constant values. Further simulation work is needed to merge the model parameters into a single set of parameters. Data from the gavage dosing study should be simulated with the model parameters for inhalation of TCE to resolve differences between model parameter estimates for each route of exposure and to delineate the influence of the corn oil vehicle on estimating model parameter estimates. Resolution of route-to-route differences in rate constant values that describe formation and metabolism of DCA remains unclear at this point because of analytical uncertainty in measuring trace quantities of metabolically formed DCA in the presence of relatively high concentrations of TCA.

Ability of the PBPK Models to Predict Pharmacokinetics of TCE and Its Metabolites in Mice

The first-generation mice PBPK models for TCE in blood and TCA in plasma were developed for gavage dosing of TCE dissolved in corn oil (*12*) and for inhalation of TCE vapors (*11*). Male and female mice were gavage dosed with either 487, 973, or 1,947 mg/kg. In other experiments female mice were exposed for 4 hr to TCE vapor concentrations of either 42, 236, 368, or 889 ppm and male mice to TCE vapor concentrations of either 110, 297, 368, or 747 ppm. The blood concentrations of TCE were not adequately simulated by the PBPK models in the gavage-dosed or vapor-exposed male and female mice. The inability of the PBPK model for TCE to predict oral uptake kinetics by a simple first-order process was attributed to a vehicle effect (corn oil). In general the PBPK model overpredicted the blood levels of TCE for inhalation. The reason for the observation was unknown.

TCA model simulations were not predictions per se but fitted simulations for gavage dosing and inhalation routes of exposure. With a 1-compartment model, fitted simulations of the production and systemic clearance of TCA were in good agreement with observed TCA plasma concentrations for both genders of gavage-dosed mice. For the TCE vapor-exposed male and female mice, the fitted simulations of TCA plasma concentrations were in agreement with experimental findings. Systemic clearance of TCA was measured for 20 hr postexposure for the vapor-exposed mice and for 44–70 hr for the gavage-dosed mice.

The second-generation male mice models were more challenging because several more metabolites were included in the model structure. For the gavage-dosed mice (*14*), model predictions were compared to observations for TCE corn oil gavage doses of 300, 600, 1,200, and 2,000 mg/kg. Model predictions for TCE and its metabolites in blood, tissues, and urine were in general agreement with observations in most simulations, but in a few cases, prediction and observation were not in close agreement. Discrepancies between model predictions and observations are expected, since the philosophy is to develop a PBPK model that is robust and can describe a wide range of data sets with a single set of model parameters. Modest model discrepancies compared to measured values were reported for clearance of TCOH from lung in the two lowest dose groups, TCA concentration in blood of the 300-mg/kg dose group, and the cumulative amount of TCA excreted in urine from the 2,000-mg/kg dose group.

Abbas and Fisher (*14*) used a single metabolic rate constant (calculated from the 1,200-mg/kg dose group) to describe formation of DCA via dechlorination of TCA in all gavage dose groups. This resulted in the slight overprediction of DCA concentrations in blood and liver in the 600- and 300-mg/kg dose groups. The authors suggested that this discrepancy between model simulation and observation might be related to the influence of the vehicle (corn oil) on the dose rate of delivery of TCE to the liver.

Greenberg et al. (*15*) exposed mice to 100 and 600 ppm of TCE vapors for 4 hr. The PBPK model was generally successful with a few exceptions in predicting the kinetic profile for TCE and its oxidative metabolites after inhalation of TCE vapors. Peak TCOH concentrations in lung tissue were underpredicted by a factor of 2 for the 100-ppm exposure group and TCOH-b systemic clearance from blood was slightly greater than predicted by the model for both exposure groups. To avoid gross overpredictions in TCE blood concentrations, fractional uptake of inhaled TCE was employed (53%). Supporting experimental evidence for fractional uptake of TCE into lung blood was obtained by conducting exhaled breath experiments. This modeling approach has been used previously for polar organic chemicals (*30*). To validate the hypothesis of fractional uptake of TCE in mice, further experiments are required in which exhaled breath is measured during inhalation of TCE in mice.

PBPK Model Structures for TCE and Its P450-Mediated Metabolites in Humans

The first-generation PBPK model for TCE in humans (*13*) was a 4-compartment

model with the same model structure as the first-generation PBPK model for mice (Figure 1). TCA was described with a classical 1-compartment model similar to the mice. In the human, the yield of TCA was accounted for by conversion of TCOH to TCA and by conversion of TCE (via CH) to TCA, which was not explicitly determined in the first-generation mouse model. The human PBPK model for TCE and its oxidative metabolite, TCA, was developed using published human pharmacokinetic data taken from controlled TCE vapor exposures and studies in which sodium trichloroacetate was administered by i.v. drip and CH and TCOH by oral administration.

In the second-generation human model (*16*), six compartments (liver, lung, kidney, and richly perfused and slowly perfused tissues) were used to describe the pharmacokinetics of TCE (Figure 2A). Only two metabolites of TCE, TCA and TCOH, were incorporated as submodels (Figure 2D) because TCA and TCOH were the only measured metabolites in blood except for intermittent trace amounts of DCA in plasma. Four compartments (body, liver, kidney, and lung) were used to describe these metabolites (Figure 2B). The TCE human model was linked to the submodels, as shown in Figure 2D. POs were used to describe the yield of TCA and TCOH, similar to the first-generation human PBPK model for TCA (Figure 1).

Derivation of PBPK Model Parameters for Humans

The first-generation model (*13*) was developed using pharmacokinetic data reported in the literature for humans. Simulations were conducted using SCoP software (National Biomedical Simulation Resource, Duke University, Durham, NC). The human V_{maxc} value (14.9 mg/kg/hr) was an optimized value based on exhaled breath (TCE), TCE blood–time-course data, and TCA concentrations in plasma and urine.

The amount of TCOH produced from TCA was estimated by pharmacokinetic analysis using TCA plasma–time-course data from two volunteers given repeated oral administration of TCOH (*31*). The volume of distribution of TCA was estimated by pharmacokinetic analysis of TCA plasma concentrations in three humans dosed with sodium TCA by i.v. drip (*32*). Published controlled TCE vapor exposures in humans were used to develop and validate the human PBPK model for TCE using exhaled breath and blood concentration data.

The second-generation PBPK model for TCE in humans was based on recent 4-hr TCE inhalation exposures conducted with nine male and eight female consenting volunteers (*16*). The whole-body exposures were conducted in a chamber described by Raymer et al. (*33*). Several blood samples were taken from each individual by venous catheter during the exposure period and for 18 hr postexposure in addition to urine samples. Alveolar breath samples were collected from a few of the exposed volunteers after the 4-hr exposure using methods described by Pleil and Lindstrom (*34*). After this period the volunteers returned to the Research Triangle Institute (Research Triangle Park, NC) once each day for 3 days to deliver their voided urine and to have blood drawn by venipuncture.

The following chemicals were analyzed for in blood and urine: TCE, CH, TCOH, TCOH-b, TCA, and DCA using methods reported by Abbas and Fisher (*14*) and by Ketcha et al. (*35*). TCE, TCOH, and TCA were found in all blood samples, TCOH-b and TCA in all urine samples, and TCE in exhaled breath samples. DCA was found intermittently above the limit of detection (> 4 µg/L) in the blood of three of nine males and two of eight females, ranging from 5 to 12 µg/L.

Blood/air partition coefficient values for TCE in the second-generation model were determined by vial equilibration (*25*) for several of the male and female volunteers (Table 4). Human tissue/air PC values for TCE were determined for lung, liver, kidney, and fat using fresh chilled tissues from donors. Other donors provided liver, kidney, muscle, and lung tissue to measure TCOH and TCA PC values in tissues. Tissue/media and blood/media PC values for TCOH and TCA were determined via a nonvolatile technique (*26*). Fresh blood was obtained from two female donors to measure the TCOH and TCA blood/media PC values.

Using the model structure in Figure 2A and physiological model parameter values given in Table 5, the optimized values for V_{maxc} (mg/kg/hr, allometrically scaled, $bw^{0.75}$) and K_m (mg/L) were obtained for each gender by fitting predicted with observed mixed venous TCE blood concentrations (Table 6). To obtain adequate model predictions of TCA and TCOH blood–time-course kinetics, the optimized V_{maxc} values were increased from 2.30 and 4.74 mg/kg/hr for males and to 4.0 and 5.0 mg/kg/hr for

Table 4. Partition coefficient values for TCE in first- and second-generation PBPK human models and for TCOH and TCA in second-generation PBPK human model.

Partition coefficient	First-generation human model	Second-generation human model	
	Male	Female	Male
Trichloroethylene			
Blood/air	9.20	9.13	11.15
Liver/blood	6.82	5.92	4.85
Kidney/blood	–[a]	1.32	1.08
Lung/blood	–[a]	0.48	0.39
Body (muscle)/blood	2.35	1.68	1.38
Fat/blood	73.3	63.88	52.34
Trichloroethanol (free)			
Liver/blood		0.59	0.59
Kidney/blood		2.15	2.15
Lung/blood		0.66	0.66
Body (muscle)/blood		0.91	0.91
Trichloroacetic acid			
Liver/blood		0.66	0.66
Kidney/blood		0.66	0.66
Lung/blood		0.47	0.47
Body (muscle)/blood		0.52	0.52

[a]Compartment was not included in the first-generation PBPK human model.

Table 5. Compartment volumes, blood flows, cardiac output, alveolar ventilation, and body weight values used in the first- and second-generation PBPK human models for TCE.

Physiological parameter	First-generation human model	Second-generation human model	
	Male	Female	Male
Compartment volumes (% bw)			
Liver	2.6	2.4	2.6
Lung	–[a]	1.4	1.4
Kidney	–[a]	0.47	0.4
Slowly perfused	62	47.0–61.0	55.0–72.0
Richly perfused	5	4.7	4.6
Fat	19	21.0–35.0	10.0–27.0
Body (for metabolites)	–[a]	92.0	92.0
Blood flow (% CO)			
Liver	26	18.7	24.0
Lung	–[a]	100.0	100.0
Kidney	–[a]	17.5	19.7
Slowly perfused	25	17.3	19.2
Richly perfused	44	39.8	32.3
Fat	5	6.7	4.8
Body (for metabolites)	–[a]	68.3	56.3
Alveolar ventilation (L/hr/kg)	12.9	18.1	18.6
Cardiac output (L/hr/kg)	15.0	17.7	15.9
Body weight (kg)	70	48.6–67.3	52.3–82.7

[a]Compartment was not included in the first-generation PBPK model for human.

females, respectively; K_m values were set to the optimized of 1.80 and 1.66, respectively.

The PO constant values for TCOH and TCA were set to 0.9 and 0.1 in males and females. That is, 90% of the oxidized TCE was converted to TCOH and 10 % to TCA. A large fraction of the TCOH is converted to TCA in humans (*31*), presumably via back conversion of TCOH to CH. This back conversion of TCOH to TCA was described as a first-order process (Table 6).

Urinary excretion of TCA and TCOH-b was variable between volunteers. This suggests that individual variability may exist in the initial metabolic step for TCE (P450 CYP2E1-mediated oxidation) or in the metabolic steps required for the formation and metabolism of its major metabolites. In addition, urinary excretion rates of the metabolites may vary between individuals. The pharmacokinetic determinants responsible for the observed variability in urinary excretion of metabolites are unknown at this time. Therefore, for the sake of simplicity, individual variability was characterized by adjusting only urinary excretion model parameters for TCOH and TCA. For each individual a fitted first-order urinary excretion rate constant was used to describe urinary excretion of TCA (Table 6). A composite, nonlinear, Michaelis-Menten velocity term was used to collectively describe glucuronidation of TCOH and urinary excretion of TCOH-b (Table 6).

Ability of the PBPK Models to Predict Pharmacokinetics of TCE and Its Metabolites in Humans

The ability of the human model to simulate the pharmacokinetics of TCE and its metabolites is briefly discussed. Exhaled breath concentrations of TCE were not adequately predicted by either the first- or second-generation human PBPK models. Exhaled breath concentrations dropped more rapidly than were predicted immediately after cessation of vapor exposure to TCE. In the first-generation model for the adult male, Allen and Fisher (*13*) obtained good agreement between model-predicted (or -fitted) and mean observed TCE concentrations in blood and TCA concentrations in plasma and the mean cumulative amount of TCA excreted in urine for volunteers exposed to TCE vapors. In the second-generation PBPK model for male and female adults (*16*), pharmacokinetic profiles for TCE and its metabolites were available for each individual. Gender-specific and individual-specific model predictions (or fits) of TCE, TCOH, and TCA in blood were in general agreement with observed data for individuals exposed to 100 ppm TCE. TCE blood concentrations were underpredicted by a factor of 2 for individuals exposed to 50 ppm TCE.

Comparison of First- and Second-Generation PBPK Models in Mice and Humans: Dosimetry of TCA

Because of the importance of TCA as a proposed ultimate carcinogen for TCE-induced liver tumors in mice, a comparison of the TCA dosimetry and model sensitivity is presented for model-predicted TCA plasma and whole-blood levels. TCA was measured in plasma for the first-generation models and in whole blood for the second-generation PBPK models. The reason for the disparity between first- and second-generation mice and human model-predicted TCA concentrations in plasma and blood, respectively, is that TCA plasma and whole-blood measurements can differ by at least 2-fold because of uptake of TCA into red blood cells (*32*).

The first- and second-generation PBPK models for male adults and male mice were compared by presenting simulation results for TCA in plasma and whole blood for a 4-hr 100-ppm vapor exposure to TCE. The human male model simulated eight individual males (*16*). Daily area-under-the-concentration curve (AUC) values for TCA in plasma or blood in humans were calculated from a 10-day simulation period. In addition, the first- and second-generation PBPK models for gavage dosing of TCE were compared by simulating TCA in plasma and whole blood for a 400-mg/kg TCE single dose.

In humans the predicted peak concentration of TCA in plasma (first-generation model) was greater than the predicted peak TCA concentration in blood (second-generation model) (Figure 3). The TCA plasma AUC value using the first-generation PKPK model was 367 mg/L/day and for the second-generation model, the blood TCA–AUC values (n = 8) ranged from 74 to 343 mg/L/day with a mean plasma value of 222 mg/L/day (Table 7).

With this TCE exposure scenario, the most sensitive first-generation human model parameter for predicting AUC for TCA in plasma was the fractional yield of TCA from TCE (0.33, Table 6). A 5% increase in this value resulted in a 4.2% increase in the TCA plasma AUC value. When all other model parameter values were individually increased by 5%, the percent change in the TCA plasma AUC was negligible. In the second-generation human PBPK model the most sensitive model parameter for predicting AUC for TCA in blood was the body (muscle)/air partition coefficient value for TCA (0.52, Table 4). A 5% increase in this value resulted in a 3.6% decrease in the TCA blood AUC value. Other model parameters in the second-generation PBPK model were not as sensitive for predicting AUC for TCA in blood.

In male B6C3F$_1$ mice, the first-generation model-predicted peak TCA plasma concentrations were higher than the second-generation model-predicted TCA blood

Table 6. Chemical-specific model parameters in humans for first-generation PBPK model (TCE and TCA) and for second-generation PBPK model (TCE, TCA, TCOH).

Model parameter for human	First-generation human model	Second-generation human model	
	Male	Female	Male
TCE			
V_{maxc} (mg/hr-kg)	14.9	5.0	4.0
K_m (mg/L)	1.5	1.66	1.80
TCA			
Volume of distribution (L)	0.34–0.0034 × bw		
Fractional yield (unitless)[a]	0.33	0.1	0.1
Urinary excretion rate constant (/hr)[a]	0.028	0.6–3.0	0.13–2.0
TCOH			
Fractional yield (unitless)	0.9	0.9	
TCOH→TCA (/hr)	10.0	10.0	
Urinary excretion rate constant (mg/hr-kg) for TCOH-b		0.4–2.2	0.35–4.0

[a]Fractional yield and urinary excretion rate constants for the first- and second-generation PBPK models are not comparable because of model structure differences.

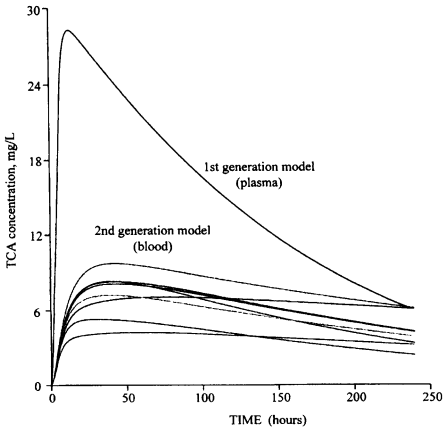

Figure 3. Computer simulation of TCA in plasma (first-generation PBPK model) and whole blood (second-generation PBPK model) resulting from a simulated 4-hr, 100-ppm constant concentration TCE vapor exposure in male humans.

Table 7. Comparison of area-under-the-plasma (first-generation model) or -blood concentration (second-generation model) curves for TCA after administration of TCE to male mice and humans.

Simulated administration of TCE	First-generation model predicted AUC for TCA in plasma (mg/L/day)	Second-generation model predicted AUC for TCA in blood (mg/L/day)
Mice (male)[a]		
Gavage (400 mg/kg)	747.0	489.0
Inhalation (100 ppm, 4 hr)	428.0	190.0
Human (male)[b]		
Inhalation (100 ppm, 4 hr)	367.0	222.0 (average) $n = 8$ 74–343 (range)

[a]Computer simulations for male mice dosed by bolus gavage with 400 mg/kg TCE or exposed to 100 ppm TCE vapors for 4 hr/day. [b]A 10-day computer simulation for male humans exposed to 100 ppm TCE for 4 hr/day.

concentrations. Figures 4 and 5 depict the simulated TCA plasma and blood–time-courses for the first- and second-generation male inhalation and gavage mice models. First-generation model-predicted AUC values for TCA in plasma were also greater than the second-generation model-predicted AUC values for TCA in blood (Table 7).

The most sensitive model parameter for the first-generation gavage model for the male mouse was the volume of distribution for TCA (0.238 L/kg, Table 3). A 5% increase in volume of distribution resulted in a 4.8% decrease in AUC value for TCA in plasma. In the first-generation male mouse inhalation model, a 5% increase in volume of distribution for TCA (0.236 L/kg, Table 3) resulted in a 4.9% decrease in the model-predicted AUC value for TCA in plasma. In addition, a 5% increase in the fractional yield of TCA from TCE (PO = 0.07, Table 3) resulted in a 4.9% increase in the AUC value for TCA in plasma. In the second-generation male mouse gavage model, blood flows to the liver and kidney (Table 1) were the most sensitive model parameters for predicting blood concentrations of TCA. The volume of the body compartment (82% bw, Table 1) and the body (muscle)/blood PC value for TCA (0.9, Table 2) were the most sensitive model parameters for predicting blood concentration of TCA in the second-generation mouse inhalation model. A 5% increase in the volume of the body compartment resulted in a 3.5% decrease in the blood concentration of TCA, and 5% increase in the body–blood PC value for TCA resulted in 3.5% increase in the blood concentration of TCA.

Summary

Several important features are present in the second-generation PBPK models for TCE in rodents and humans. These models account for additional metabolites in mice and humans that are toxicologically relevant. Model validation in mice included analyzing tissues for TCE and its metabolites in addition to blood or plasma. The first-generation models relied only on plasma and blood–time-course data. New human pharmacokinetic data were collected for the second-generation human model. These pharmacokinetic data sets were extensive and relied on improved analytical chemistry methods. DCA was identified as a minor metabolite of TCE in some individuals. Significant variability in metabolite profiles in blood and urine was found between individuals exposed to similar concentrations of TCE. This finding suggests that the dosimetry of TCE and its metabolites is more variable in humans than in experimental rodents. However, this variability can be quantified and incorporated into human PBPK models intended for risk assessment.

The second-generation PBPK models for TCE describe the pharmacokinetics of TCE and its P450-mediated metabolites using a complex metabolic scheme, which accounts for species differences. Although significant progress has been attained in formulating mathematical models to quantitatively describe the uptake and metabolism of TCE in rodents and humans, further laboratory studies and modeling efforts are warranted. Lack of knowledge about mechanisms of action for the observed toxicity caused by TCE in laboratory animals and humans remains the greatest barrier to direct implementation of the PBPK models for risk assessment purposes. PBPK modeling of the glutathione pathway for TCE warrants further attention beyond the efforts presented by Clewell et al. (*18*) to reduce the uncertainty associated with dose–response analysis of kidney tumors. Time-course kinetic studies are needed for this metabolic pathway. Studies are needed to determine what physiological or biochemical factors are responsible for the observed human variability in urinary excretion of TCOH-b and TCA (*16*). DCA has been reported as a metabolite in rodents and now humans. Analytical difficulties in the analysis of DCA in biological tissues (*35*) have recently been reported as errata to published articles (*29,36*). Further research is needed to determine the origin of DCA in rodents and humans administered or exposed to TCE. Recently, Beland et al. (*37*) reported that DCA was not produced in mice and rats administered CH. However, Muralidhara and Bruckner (*38*) reported significant amounts of DCA formation in mice dosed with TCE. Further research is needed to better understand the role of TCOH and CH in lung tumor formation of mice exposed to TCE vapors.

The PBPK models for TCE and its glutathione and P450 metabolites should be integrated into a single PBPK model for the risk assessment of TCE. Critical features of each model should be retained and the PBPK model should be constructed with a priori assumptions about extrapolation requirements. In summary, substantial advances have occurred over the last 10 years in understanding the dosimetry of TCE and its metabolites in rodents and humans. These advances in PBPK modeling can be used today in crafting scientifically sound public health decisions for TCE.

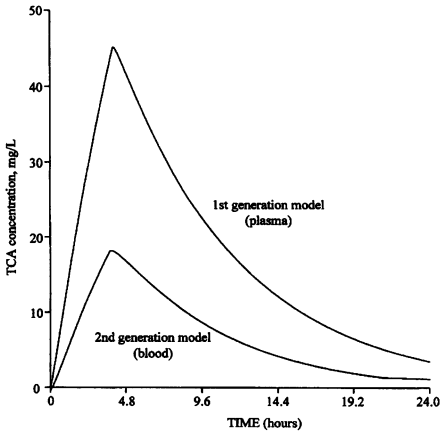

Figure 4. Computer simulation of TCA in plasma (first-generation PBPK model) and whole blood (second-generation PBPK model) resulting from a simulated 4-hr, 100-ppm constant concentration TCE vapor exposure in male mice.

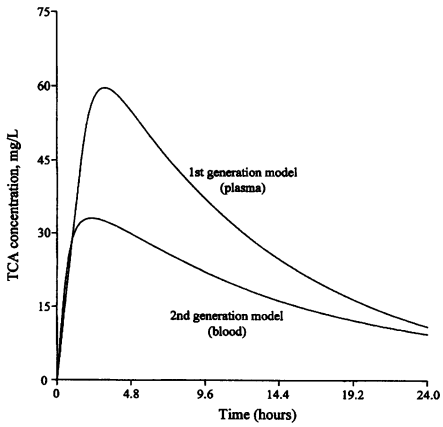

Figure 5. Computer simulation of TCA in plasma (first-generation PBPK model) and whole blood (second-generation PBPK model) resulting from a simulated 400-mg/kg bolus gavage dose of TCE in male mice.

References and Notes

1. Sato A, Nakajima T, Fujiwara Y, Murayama N. A pharmacokinetic model to study the excretion of trichloroethylene and its metabolites after an inhalation exposure. Br J Ind Health 34:56–63 (1977).
2. Fernandez JG, Droz PO, Humbert BE, Caperous JR. Trichloroethylene exposure: simulation of uptake , excretion, and metabolism using a mathematical model. Br J Ind Med 34:43–55 (1977).
3. Andersen ME, Gargas ML, Clewell HJ III, Severyn KM. Quantitative evaluation of the metabolic interactions between trichloroethylene and 1,2-dichloroethylene *in vivo* using gas uptake methods. Toxicol Appl Pharmacol 89:149–157 (1987).
4. Dallas CE, Gallo JM, Ramanathan R, Muralidhara S, Bruckner J. Physiological pharmacokinetic modeling of inhaled trichlorethylene in rats. Toxicol Appl Pharmacol 110:303–314 (1991).
5. Bogen KT. Pharmacokinetics for regulatory analysis: the case of trichloroethylene. Regul Toxicol Pharmacol 8:447–466 (1988).
6. U.S. EPA. Health Assessment Document for Trichloroethylene. EPA 600/8-82-/006F, PB-249696. Washington, DC:U.S. Environmental Protection Agency, 1985.
7. Koizumi A. Potential of physiologically based pharmacokinetics to amalgamate kinetic data of trichloroethylene and tetrachloroethylene obtained in rats and man. Br J Ind Med 46:239–249 (1989).
8. Fisher JW, Whittaker TA, Taylor DH, Clewell HJ III, Andersen ME. Physiologically based pharmacokinetic modeling of the pregnant rat: a multiroute exposure model for trichloroethylene and its metabolite, trichloroacetic acid. Toxicol Appl Pharmacol 99:395–414 (1989).
9. Fisher JW, Whittaker TA, Taylor DH, Clewell HJ III, Andersen ME. Physiologically based pharmacokinetic modeling of the lactating rat and nursing pup: a multiroute exposure model for trichloroethylene and its metabolite, trichloroacetic acid. Toxicol Appl Pharmacol 102:497–515 (1990).
10. Herren-Freund, SL, Pereira, MA, Khoury, MD, Olson, G. The carcinogenicity of trichloroethylene and its metabolites, trichloroacetic acid and dichloroacetic acid, in mouse liver. Toxicol Appl Pharmacol 90:183–189 (1987).
11. Fisher JW, Gargas ML, Allen BC, Andersen ME. Physiologically based pharmacokinetic modeling with trichloroethylene and its metabolites, trichloroacetic acid, in the rat and mouse. Toxicol Appl Pharmacol 109:183–195 (1991).
12. Fisher JW, Allen BC. Evaluating the risk of liver cancer in humans exposed to trichloroethylene using physiological models. Risk Anal 13:87–95 (1993).
13. Allen BC, Fisher JW. Pharmacokinetic modeling of trichloroethylene and trichloroacetic acid in humans. Risk Anal 13:71–86 (1993).
14. Abbas R, Fisher JW. A physiologically based pharmacokinetic model for trichloroethylene and its metabolites, chloral hydrate, trichloroacetate, dichloroacetate, trichloroethanol, trichloroethanol glucuronide in B6C3F1 mice. Toxicol Appl Pharmacol 147:15–30 (1997).
15. Greenberg, MS, Burton, Jr. GA, and Fisher JW. Physiologically based pharmacokinetic modeling of inhaled trichloroethylene and its oxidative metabolites in B6C3F1 mice. Toxicol Appl Pharmacol 154:264–278 (1999).
16. Fisher JW, Mahle DA, Abbas R. A human physiologically based pharmacokinetic model for trichloroethylene and its metabolites, trichloroacetic acid and free trichloroethanol. Toxicol Appl Pharmacol 152:339–359 (1998).
17. Cronin WC IV, Oswald EJ, Shelley ML, Fisher JW, Flemming CD. A trichloroethylene risk assessment using a Monte Carlo analysis of parameter uncertainty in conjunction with physiologically-based pharmacokinetic modeling. Risk Anal 15:555–565 (1995).
18. Clewell HJ, Gentry PR, Gearhart JM, Allen BC, Andersen ME. Considering pharmacokinetic and mechanistic information in cancer risk assessments for environmental contaminants: examples with vinyl chloride and trichloroethylene. Chemosphere 31:2561–2578 (1995).
19. Bogen KT, Gold LS. Trichloroethylene cancer risk: simplified calculation of PBPK-based MCLs for cytotoxic endpoints. Regul Toxicol Pharmacol 25:26–42 (1997).
20. Simon T. Combining physiologically based pharmacokinetic modeling with Monte Carlo simulation to derive an acute inhalation guidance value for trichloroethylene. Regul Toxicol Pharmacol 26:257–270 (1997).
21. Ramsey JC, Andersen ME. A physiologically based description of the inhalation pharmacokinetics of styrene in rats and humans. Toxicol Appl Pharmacol 73:159–175 (1984).
22. U.S. EPA. Addendum to the Health Assessment Document for Trichloroethylene: Updated Carcinogencity Assessment for Trichloroethylene. Draft. EPA/600/8-82/006FA. Washington, DC:U.S. Environmental Protection Agency, 1987.
23. Davidson IWF, Beliles RP. Consideration of the target organ toxicity of trichloroethylene in terms of metabolite toxicity and pharmacokinetics. Drug Metab Rev 23(5&6):493–599 (1991).
24. Larson JL, Bull RJ. Metabolism and lipoperoxidative activity of trichloroacetate and dichloroacetate in rats and mice. Toxicol App Pharmacol 115:268–277 (1992).
25. Gearhart JM, Mahle DA, Greene RJ, Seckel CS, Flemming CD, Fisher JW, Clewell HA III. Variability of physiologically based pharmacokinetic (PB-PK) model parameters and their effects on PB-PK model predictions in a risk assessment for perchloroethylene (PCE). Toxicol Lett 68:131–144 (1993).
26. Jepson GW, Hoover DK, Black RK, McCafferty JD, Mahle DA, Gearhart JM. A partition coefficient method for non-volatile and intermediate volatility chemicals in biological tissues. Fundam Appl Toxicol 22:519–524 (1994).
27. Abbas R, Seckel CS, MacMahon KL, Fisher JW. Determination of kinetic rate constants for chloral hydrate, trichloroethanol, trichloroacetic acid, and dichloroacetic acid—a physiologically based modeling approach. Toxicologist 36:32 (1997).
28. Abbas R, Seckel CS, MacMahon KL, Kidney JK, Fisher JW. Pharmacokinetic analysis of chloral hydrate and its metabolism in B6C3F1 mice. Drug Metab Dispos 24:1340–1346 (1996).
29. Fisher JW. Erratum (1997) to Abbas et al. Drug Metab Dispos 25(12):1449 (1996).
30. Johanson G. Modeling of respiratory exchange of polar solvents. Ann Occup Hyg 35:323–339 (1991).
31. Marshall EK, Owens AH Jr. Absorption excretion, and metabolic fate of chloral hydrate and trichloroethanol. Bull Johns Hopkins Hosp 95:1–18 (1954).
32. Paykoc ZV, Powell JF. The excretion of sodium trichloroacetate. J Pharmacol Exp Ther 85:289–293 (1945).
33. Raymer JH, Kizakevich ML, McCartney ML, Pellizzari ED. Facilities for human exposure studies. Environ Sci Technol 27:1733–1735 (1993).
34. Pleil JD, Lindstrom AB. Collection of a single alveolar breath for volatile compounds analysis. Am J Ind Med 28:109–121 (1995).
35. Ketcha MM, Warren DA, Bishop CT, Brashear WT. Factors influencing the conversion of trichloroacetic acid to dichloroacetic acid in biological matrices. J Anal Toxicol 20:236–241 (1996).
36. Erratum (1995) to Templin et al. Toxicol Appl Pharmacol 133:177 (1993).
37. Beland FA, Schmitt TC, Fullerton NF, Young JF. Metabolism of chloral hydrate in mice and rats after single and multiple doses. J Toxicol Environ Health 54:209–226 (1998).
38. Muralidhara S, Bruckner JV. Simple method for rapid measurement of trichloroethylene and its major metabolites in biological samples. J Chromatog B 732:145–153 (1999).